

Appendix for Submission # 6611

A Additional Verification for Empirical Studies

In this section, we provide additional verification of our empirical studies (Sec.2.2) and INR representation experiments (Sec.4.1). We conduct experiments on the Kodak dataset [14], maintaining all configurations identical to those described in Sec. 4.1. The quantitative results are presented in Tab. 4. The configurations Standard, Bias Free, H_1 Bias, Output Bias, and Input Bias align with those in Tab. 1. Additionally, we include H_2 Bias and H_3 Bias, representing networks with bias terms exclusively in the second and third layers, respectively. Settings without underlines represent standard SIREN implementations, while underlined settings correspond to FINER. The symbol \odot indicates reconstructions exhibiting *spatial aliasing*. For each configuration block, we report averaged metrics both with and without bias term backpropagation. Complementary results on the DIV2K dataset are presented in Tab. 5, supplementing the findings in Tab. 1. The results in Tab. 5 and Tab. 4 further validate our observations from Sec. 2.2 and conclusions from Sec. 4.1. These findings substantiate both the magnitude of bias terms' impact in INRs and the effects of their gradient optimization, lending additional support to Proposition 1. This reinforces our claim that the primary role of bias terms in neural representations is to eliminate *spatial aliasing* arising from the symmetry of coordinate space and activation functions.

Table 4: Results of 2D image fitting tasks with varying bias configurations (Kodak dataset)

Settings	1k Iterations		3k Iterations		5k Iterations	
	PSNR \uparrow	SSIM \uparrow	PSNR \uparrow	SSIM \uparrow	PSNR \uparrow	SSIM \uparrow
Standard	30.05 / 30.05	0.832 / 0.832	33.93 / 33.92	0.912 / 0.912	35.24 / 35.23	0.929 / 0.929
Bias Free \odot	15.06 / 15.06	0.599 / 0.599	15.09 / 15.09	0.620 / 0.620	15.10 / 15.10	0.626 / 0.626
H_1 Bias	29.67 / 29.68	0.822 / 0.822	33.25 / 33.25	0.902 / 0.902	34.44 / 34.45	0.919 / 0.919
H_2 Bias	29.96 / 29.96	0.831 / 0.831	33.33 / 33.32	0.903 / 0.903	34.41 / 34.42	0.918 / 0.918
H_3 Bias	30.07 / 30.05	0.829 / 0.829	33.17 / 33.16	0.895 / 0.894	34.18 / 33.17	0.910 / 0.910
Output Bias \odot	16.34 / 16.04	0.613 / 0.610	17.03 / 16.78	0.641 / 0.639	17.31 / 17.02	0.648 / 0.646
Input Bias	30.78 / 30.78	0.854 / 0.854	34.31 / 34.30	0.917 / 0.917	35.42 / 35.42	0.930 / 0.930
<u>Standard</u>	32.05 / 32.06	0.880 / 0.881	36.18 / 36.18	0.940 / 0.940	37.52 / 37.53	0.952 / 0.952
<u>Bias Free\odot</u>	15.09 / 15.09	0.617 / 0.617	15.11 / 15.11	0.632 / 0.632	15.11 / 15.11	0.636 / 0.636
<u>H_1 Bias</u>	30.83 / 30.82	0.853 / 0.853	34.46 / 34.45	0.921 / 0.921	35.82 / 35.81	0.935 / 0.935
<u>H_2 Bias</u>	31.28 / 31.28	0.866 / 0.866	34.74 / 34.75	0.924 / 0.924	35.66 / 35.67	0.934 / 0.935
<u>H_3 Bias</u>	31.37 / 31.36	0.865 / 0.864	34.60 / 34.60	0.919 / 0.919	35.60 / 35.59	0.931 / 0.931
<u>Output Bias\odot</u>	16.19 / 16.07	0.628 / 0.627	16.82 / 16.79	0.652 / 0.651	17.10 / 17.04	0.655 / 0.657
<u>Input Bias</u>	33.06 / 33.05	0.901 / 0.900	36.81 / 36.80	0.948 / 0.950	37.92 / 37.91	0.955 / 0.955

Table 5: Results of 2D image fitting tasks with varying bias configurations (DIV2K dataset)

Settings	1k Iterations		3k Iterations		5k Iterations	
	PSNR \uparrow	SSIM \uparrow	PSNR \uparrow	SSIM \uparrow	PSNR \uparrow	SSIM \uparrow
Standard	30.30 / 30.30	0.882 / 0.882	34.68 / 34.69	0.946 / 0.946	36.17 / 36.18	0.956 / 0.959
Bias Free \odot	13.98 / 13.98	0.556 / 0.556	14.00 / 14.00	0.574 / 0.574	14.03 / 14.03	0.577 / 0.577
H_1 Bias	29.88 / 29.87	0.872 / 0.872	34.02 / 34.00	0.938 / 0.938	35.33 / 35.34	0.950 / 0.950
H_2 Bias	30.14 / 30.13	0.875 / 0.875	33.98 / 33.96	0.935 / 0.935	35.20 / 35.19	0.946 / 0.946
H_3 Bias	30.18 / 30.14	0.871 / 0.869	33.65 / 33.63	0.927 / 0.926	34.77 / 34.76	0.934 / 0.933
Output Bias \odot	14.67 / 14.49	0.567 / 0.562	15.11 / 14.96	0.593 / 0.583	15.11 / 15.13	0.586 / 0.588
Input Bias	31.20 / 31.18	0.903 / 0.902	35.33 / 35.32	0.953 / 0.953	36.61 / 36.63	0.962 / 0.962
<u>Standard</u>	32.26 / 32.25	0.916 / 0.916	36.84 / 36.83	0.962 / 0.962	38.47 / 38.47	0.971 / 0.971
<u>Bias Free\odot</u>	13.99 / 13.99	0.568 / 0.568	14.01 / 14.01	0.581 / 0.581	14.03 / 14.03	0.583 / 0.583
<u>H_1 Bias</u>	31.06 / 31.08	0.894 / 0.894	35.21 / 35.23	0.950 / 0.949	36.63 / 36.62	0.958 / 0.958
<u>H_2 Bias</u>	31.49 / 31.49	0.901 / 0.901	35.28 / 35.24	0.948 / 0.947	36.62 / 36.60	0.957 / 0.957
<u>H_3 Bias</u>	31.66 / 31.60	0.901 / 0.899	35.21 / 35.18	0.946 / 0.944	36.32 / 36.30	0.952 / 0.951
<u>Output Bias\odot</u>	14.55 / 14.51	0.577 / 0.573	15.13 / 14.98	0.599 / 0.590	15.22 / 15.14	0.595 / 0.594
<u>Input Bias</u>	33.39 / 33.38	0.933 / 0.932	37.95 / 37.90	0.968 / 0.968	39.30 / 39.29	0.974 / 0.974

B Additional Experiments for Feat-Bias

In this section, we present additional experiments to validate the effectiveness of Feat-Bias (Sec.3). Following prior work[59, 19, 15], we evaluate our method on INR classification tasks using MNIST and F-MNIST datasets. In addition to the baselines discussed in Sec.D, we include comparisons with recent methods including Inr2Vec[28], DWS [33], and NG-GNN [23]. Feat-Bias_[ViT] and Feat-Bias_[DINOv2] represent our method using features extracted from ViT [10] and DINOv2 [34], respectively. We maintain identical configurations as described in Sec. D, employing a 3×256 MLP downstream network, training for 1000 iterations with a cosine scheduler and learning rate of $1e-3$. The quantitative results are presented in Tab. 6. Our Feat-Bias_[DINOv2] achieves the highest classification accuracy on both datasets, surpassing the recent state-of-the-art MWT-L. Notably, on F-MNIST, our method improves accuracy from 87.32% to 92.38%, demonstrating significant advancement in INR downstream tasks.

Table 6: INR classification on MNIST and Fashion-MNIST Datasets

Method	MNIST	F-MNIST	Method	MNIST	F-MNIST
MLP	17.55±0.01	19.91±0.47	Inr2Vec [28]	23.69±0.10	22.33±0.41
NFN _{NP} [59]	78.50±0.23	68.19±0.28	NFN _{HNP} [59]	79.11±0.84	68.94±0.64
DWS [33]	85.71±0.57	67.06±0.29	NG-GNN [23]	91.40±0.60	68.00±0.20
ScaleGMN [19]	96.57±0.10	80.46±0.32	ScaleGMN-B [19]	96.59±0.24	80.78±0.16
WT [15]	93.08±2.26	73.81±1.43	MWT _{Mid-Task} [15]	95.57±0.30	77.23±0.56
MWT [15]	96.58±0.32	83.86±0.91	MWT-L [15]	98.33±0.13	87.32±0.16
Feat-Bias _[ViT]	95.79±0.04	90.13±0.49	Feat-Bias _[DINOv2]	98.48±0.05	92.38±0.06

C Additional Experiments for Ablation Studies

We present additional ablation studies to further verify the source of *spatial aliasing*. All experimental settings strictly align with those in Sec. 4.3. Tab 7 present ablation result for spatial aliasing on Kodak dataset, demonstrating consistency with the findings presented in Tab. 3.

Table 7: Ablation study for *spatial aliasing* (Kodak Dataset)

Settings	standard	w/o coord. sym.	w/o act. sym. (+1)	w/o act. sym. (−1)
Full-Bias	35.23 / 0.929 / 0.089	32.23 / 0.880 / 0.191	30.38 / 0.838 / 0.257	30.44 / 0.840 / 0.254
Bias-Free	15.10 / 0.626 / 0.461	32.17 / 0.877 / 0.200	30.11 / 0.832 / 0.258	30.11 / 0.832 / 0.259

D Additional Experiments for classification task

Experimental Settings. In this section, we further evaluate the effectiveness of our proposed Feat-Bias (Sec. 3) on INR downstream tasks. The downstream network of Feat-Bias consists of a lightweight 3×256 MLP classifier. Since the CIFAR-100 dataset is more complex than CIFAR-10, the number of iterations is changed to 5000, using a cosine scheduler with a learning rate of $1e-3$. In addition, the iteration count of MWT has also been modified to 20 epochs. In tab 8, we list the performance metrics at 10 epochs (i.e., the original default setting) and 20 epochs. All experiments are repeated three times, reporting both mean and standard deviation.

Quantitative Results. Tab. 8 shows the classification results for CIFAR-100 dataset [24], where we also adopt Implicit-Zoo’s default configuration with a 1×64 SIREN network like the settings in the main text to ensure consistent experimental conditions across all comparisons. Since Implicitly Zoo does not provide the INR dataset of CIFAR-100, only MWT is compared with our method here. As evidenced by the results, our method achieves superior performance across accuracy, precision, and F1 score metrics meanwhile greatly reduces the training time, further demonstrating Feat-Bias’s effectiveness in INR post-processing tasks.

Table 8: INR classification on CIFAR-100 Datasets

Method	<i>Classification Task</i>					<i>INRs</i>	
	Accuracy (%) \uparrow	Precision (%) \uparrow	F1 \uparrow	Time \downarrow	Params (kilo #) \downarrow	PSNR (dB) \uparrow	SSIM \uparrow
WT _{10epochs} [15]	12.21 \pm 0.89	10.90 \pm 0.62	10.09 \pm 0.87	73.52 \pm 1.78 (min)	261	32.33	0.942
WT _{20epochs} [15]	15.83 \pm 0.71	13.82 \pm 0.85	13.84 \pm 0.79	151.78 \pm 2.93 (min)	261	34.89	0.964
MWT _{Mid-Task-10epochs} [‡] [15]	15.81 \pm 0.44	14.94 \pm 0.86	13.86 \pm 0.74	83.41 \pm 1.55 (min)	261	30.17	0.910
MWT _{Mid-Task-20epochs} [‡] [15]	19.87 \pm 0.21	17.88 \pm 0.11	18.06 \pm 0.15	169.42 \pm 2.80 (min)	261	33.06	0.948
MWT _{10epochs} [15]	19.46 \pm 0.88	18.09 \pm 0.58	17.67 \pm 0.69	83.74 \pm 0.97 (min)	261	24.45	0.752
MWT _{20epochs} [15]	23.29 \pm 0.57	21.56 \pm 0.67	21.78 \pm 0.65	168.0 \pm 1.27 (min)	261	25.80	0.806
Feat-Bias _[ViT]	74.83 \pm 0.07	75.03 \pm 0.09	74.79 \pm 0.07	144.70 \pm 1.83 (sec)	151	/	/
Feat-Bias _[DINOv2]	78.51 \pm 0.16	78.71 \pm 0.13	78.46 \pm 0.15	145.38 \pm 1.65 (sec)	151	/	/

[‡] denotes ω_{task} reported in MWT [15].

389 **E Additional visualizations for *spatial aliasing***

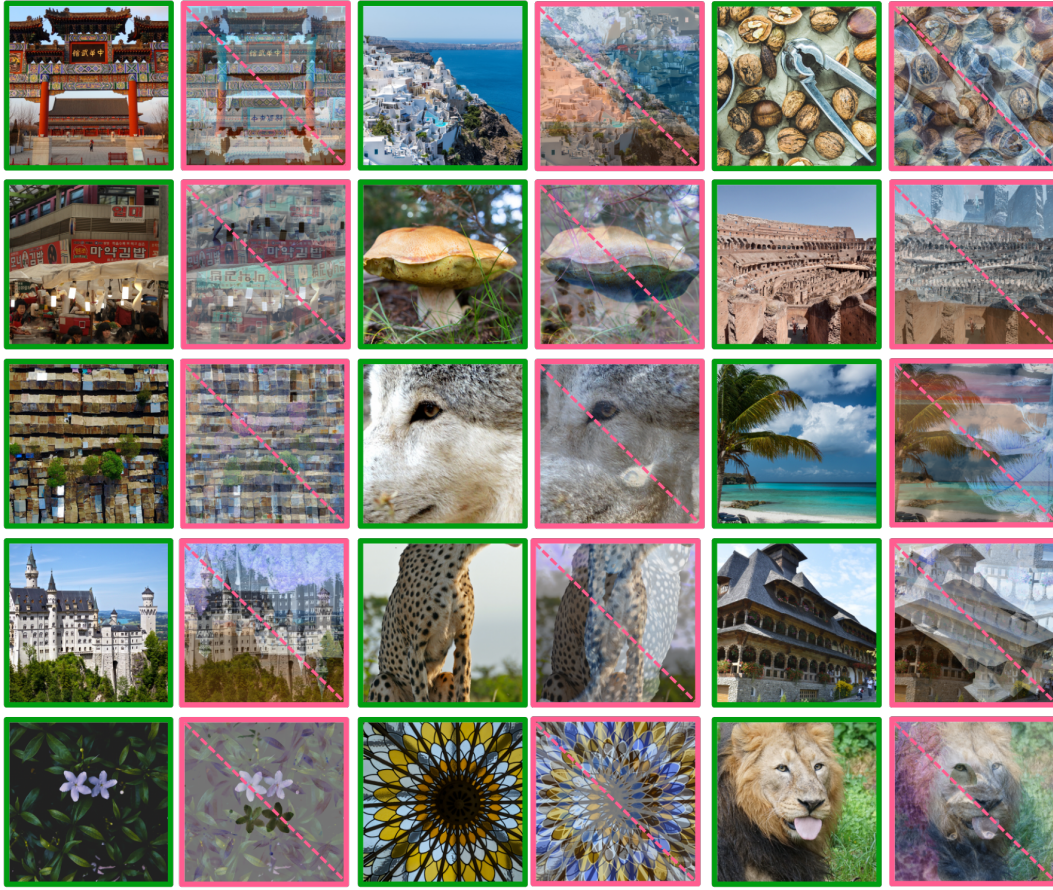


Figure 5: Visualization for *spatial aliasing*: reconstructed signals demonstrate central symmetry, manifesting as aliasing artifacts between distinct regions of the input. Green and Pink denote the ground truth and reconstructed signals with *spatial aliasing*, respectively.

References

- [1] Eirikur Agustsson and Radu Timofte. Ntire 2017 challenge on single image super-resolution: Dataset and study. In *Proceedings of the IEEE conference on computer vision and pattern recognition workshops*, pages 126–135, 2017.
- [2] Hmrishav Bandyopadhyay, Ayan Kumar Bhunia, Pinaki Nath Chowdhury, Aneeshan Sain, Tao Xiang, Timothy M. Hospedales, and Yi-Zhe Song. Sketchinr: A first look into sketches as implicit neural representations. *CoRR*, abs/2403.09344, 2024.
- [3] Nuri Benbarka, Timon Höfer, Hamd ul Moqeet Riaz, and Andreas Zell. Seeing implicit neural representations as fourier series. In *WACV*, pages 2283–2292. IEEE, 2022.
- [4] Anpei Chen, Zexiang Xu, Andreas Geiger, Jingyi Yu, and Hao Su. Tensorf: Tensorial radiance fields. In *European conference on computer vision*, pages 333–350. Springer, 2022.
- [5] Hao Chen, Bo He, Hanyu Wang, Yixuan Ren, Ser-Nam Lim, and Abhinav Shrivastava. Nerv: Neural representations for videos. In *NeurIPS*, pages 21557–21568, 2021.
- [6] Xiang Chen, Jinshan Pan, and Jiangxin Dong. Bidirectional multi-scale implicit neural representations for image deraining. In *CVPR*, pages 25627–25636. IEEE, 2024.
- [7] Yinbo Chen and Xiaolong Wang. Transformers as meta-learners for implicit neural representations. In *ECCV (17)*, volume 13677 of *Lecture Notes in Computer Science*, pages 170–187. Springer, 2022.
- [8] Junwoo Cho, Seungtae Nam, Hyunmo Yang, Seok-Bae Yun, Youngjoon Hong, and Eunbyung Park. Separable physics-informed neural networks. In *NeurIPS*, 2023.
- [9] Tomás Chobola, Yu Liu, Hanyi Zhang, Julia A. Schnabel, and Tingying Peng. Fast context-based low-light image enhancement via neural implicit representations. In *ECCV (86)*, volume 15144 of *Lecture Notes in Computer Science*, pages 413–430. Springer, 2024.
- [10] Alexey Dosovitskiy, Lucas Beyer, Alexander Kolesnikov, Dirk Weissenborn, Xiaohua Zhai, Thomas Unterthiner, Mostafa Dehghani, Matthias Minderer, Georg Heigold, Sylvain Gelly, Jakob Uszkoreit, and Neil Houlsby. An image is worth 16x16 words: Transformers for image recognition at scale. In *ICLR*. OpenReview.net, 2021.
- [11] Emilien Dupont, Adam Goliński, Milad Alizadeh, Yee Whye Teh, and Arnaud Doucet. Coin: Compression with implicit neural representations. *arXiv preprint arXiv:2103.03123*, 2021.
- [12] Emilien Dupont, Hyunjik Kim, S. M. Ali Eslami, Danilo Jimenez Rezende, and Dan Rosenbaum. From data to functa: Your data point is a function and you can treat it like one. In *ICML*, volume 162 of *Proceedings of Machine Learning Research*, pages 5694–5725. PMLR, 2022.
- [13] Emilien Dupont, Hrushikesh Loya, Milad Alizadeh, Adam Golinski, Yee Whye Teh, and Arnaud Doucet. COIN++: neural compression across modalities. *Trans. Mach. Learn. Res.*, 2022, 2022.
- [14] E.Kodak. Kodak dataset, 1999.
- [15] Alexander Gielisse and Jan van Gemert. End-to-end implicit neural representations for classification. *CVPR*, 2025.
- [16] Ian Goodfellow, Yoshua Bengio, Aaron Courville, and Yoshua Bengio. *Deep learning*, volume 1. MIT press Cambridge, 2016.
- [17] Jiajun He, Gergely Flamich, Zongyu Guo, and José Miguel Hernández-Lobato. RECOMBINER: robust and enhanced compression with bayesian implicit neural representations. In *ICLR*. OpenReview.net, 2024.
- [18] Langwen Huang and Torsten Hoefer. Compressing multidimensional weather and climate data into neural networks. In *ICLR*. OpenReview.net, 2023.
- [19] Ioannis Kalogeropoulos, Giorgos Bouritsas, and Yannis Panagakis. Scale equivariant graph metanetworks. In *NeurIPS*, 2024.

- [20] Namgyu Kang, Jaemin Oh, Youngjoon Hong, and Eunbyung Park. PIG: physics-informed gaussians as adaptive parametric mesh representations. *CoRR*, abs/2412.05994, 2024.
- [21] Amirhossein Kazerooni, Reza Azad, Alireza Hosseini, Dorit Merhof, and Ulas Bagci. INCODE: implicit neural conditioning with prior knowledge embeddings. In *WACV*, pages 1287–1296. IEEE, 2024.
- [22] Shakiba Kheradmand, Daniel Rebain, Gopal Sharma, Hossam Isack, Abhishek Kar, Andrea Tagliasacchi, and Kwang Moo Yi. Accelerating neural field training via soft mining. In *Proceedings of the IEEE/CVF Conference on Computer Vision and Pattern Recognition*, pages 20071–20080, 2024.
- [23] Miltiadis Kofinas, Boris Knyazev, Yan Zhang, Yunlu Chen, Gertjan J. Burghouts, Efstratios Gavves, Cees G. M. Snoek, and David W. Zhang. Graph neural networks for learning equivariant representations of neural networks. In *ICLR*. OpenReview.net, 2024.
- [24] Alex Krizhevsky, Geoffrey Hinton, et al. Learning multiple layers of features from tiny images. 2009.
- [25] Zhemin Li, Hongxia Wang, and Deyu Meng. Regularize implicit neural representation by itself. In *CVPR*, pages 10280–10288. IEEE, 2023.
- [26] Zhiheng Li, Muheng Li, Jixuan Fan, Lei Chen, Yansong Tang, Jiwen Lu, and Jie Zhou. Learning dual-level deformable implicit representation for real-world scale arbitrary super-resolution. In *ECCV (69)*, volume 15127 of *Lecture Notes in Computer Science*, pages 352–368. Springer, 2024.
- [27] Zhen Liu, Hao Zhu, Qi Zhang, Jingde Fu, Weibing Deng, Zhan Ma, Yanwen Guo, and Xun Cao. FINER: flexible spectral-bias tuning in implicit neural representation by variable-periodic activation functions. *CoRR*, abs/2312.02434, 2023.
- [28] Luca De Luigi, Adriano Cardace, Riccardo Spezialetti, Pierluigi Zama Ramirez, Samuele Salti, and Luigi Di Stefano. Deep learning on implicit neural representations of shapes. In *ICLR*. OpenReview.net, 2023.
- [29] Qi Ma, Danda Pani Paudel, Ender Konukoglu, and Luc Van Gool. Implicit zoo: A large-scale dataset of neural implicit functions for 2d images and 3d scenes. In *NeurIPS*, 2024.
- [30] Ben Mildenhall, Pratul P. Srinivasan, Matthew Tancik, Jonathan T. Barron, Ravi Ramamoorthi, and Ren Ng. Nerf: Representing scenes as neural radiance fields for view synthesis. In *ECCV (I)*, volume 12346 of *Lecture Notes in Computer Science*, pages 405–421. Springer, 2020.
- [31] Amirali Molaei, Amirhossein Aminimehr, Armin Tavakoli, Amirhossein Kazerooni, Bobby Azad, Reza Azad, and Dorit Merhof. Implicit neural representation in medical imaging: A comparative survey. In *ICCV (Workshops)*, pages 2373–2383. IEEE, 2023.
- [32] Thomas Müller, Alex Evans, Christoph Schied, and Alexander Keller. Instant neural graphics primitives with a multiresolution hash encoding. *ACM Trans. Graph.*, 41(4):102:1–102:15, 2022.
- [33] Aviv Navon, Aviv Shamsian, Idan Achituve, Ethan Fetaya, Gal Chechik, and Haggai Maron. Equivariant architectures for learning in deep weight spaces. In *ICML*, volume 202 of *Proceedings of Machine Learning Research*, pages 25790–25816. PMLR, 2023.
- [34] Maxime Oquab, Timothée Darcet, Théo Moutakanni, Huy V. Vo, Marc Szafraniec, Vasil Khalidov, Pierre Fernandez, Daniel Haziza, Francisco Massa, Alaaeldin El-Nouby, Mido Assran, Nicolas Ballas, Wojciech Galuba, Russell Howes, Po-Yao Huang, Shang-Wen Li, Ishan Misra, Michael Rabbat, Vasu Sharma, Gabriel Synnaeve, Hu Xu, Hervé Jégou, Julien Mairal, Patrick Labatut, Armand Joulin, and Piotr Bojanowski. Dinov2: Learning robust visual features without supervision. *Trans. Mach. Learn. Res.*, 2024, 2024.
- [35] Jeong Joon Park, Peter R. Florence, Julian Straub, Richard A. Newcombe, and Steven Lovegrove. DeepSDF: Learning continuous signed distance functions for shape representation. In *CVPR*, pages 165–174. Computer Vision Foundation / IEEE, 2019.

- [36] Adam Paszke, Sam Gross, Francisco Massa, Adam Lerer, James Bradbury, Gregory Chanan, Trevor Killeen, Zeming Lin, Natalia Gimelshein, Luca Antiga, Alban Desmaison, Andreas Köpf, Edward Z. Yang, Zachary DeVito, Martin Raison, Alykhan Tejani, Sasank Chilamkurthy, Benoit Steiner, Lu Fang, Junjie Bai, and Soumith Chintala. Pytorch: An imperative style, high-performance deep learning library. In *NeurIPS*, pages 8024–8035, 2019.
- [37] Nasim Rahaman, Aristide Baratin, Devansh Arpit, Felix Draxler, Min Lin, Fred A. Hamprecht, Yoshua Bengio, and Aaron C. Courville. On the spectral bias of neural networks. In *ICML*, volume 97 of *Proceedings of Machine Learning Research*, pages 5301–5310. PMLR, 2019.
- [38] Maziar Raissi, Paris Perdikaris, and George E. Karniadakis. Physics-informed neural networks: A deep learning framework for solving forward and inverse problems involving nonlinear partial differential equations. *J. Comput. Phys.*, 378:686–707, 2019.
- [39] Sameera Ramasinghe and Simon Lucey. Beyond periodicity: Towards a unifying framework for activations in coordinate-mlps. In *ECCV (33)*, volume 13693 of *Lecture Notes in Computer Science*, pages 142–158. Springer, 2022.
- [40] Simone Saitta, Marcello Carioni, Subhadip Mukherjee, Carola-Bibiane Schönlieb, and Alberto Redaelli. Implicit neural representations for unsupervised super-resolution and denoising of 4d flow MRI. *Comput. Methods Programs Biomed.*, 246:108057, 2024.
- [41] Vishwanath Saragadam, Daniel LeJeune, Jasper Tan, Guha Balakrishnan, Ashok Veeraraghavan, and Richard G. Baraniuk. WIRE: wavelet implicit neural representations. In *CVPR*, pages 18507–18516. IEEE, 2023.
- [42] Vishwanath Saragadam, Jasper Tan, Guha Balakrishnan, Richard G. Baraniuk, and Ashok Veeraraghavan. MINER: multiscale implicit neural representation. In *ECCV (23)*, volume 13683 of *Lecture Notes in Computer Science*, pages 318–333. Springer, 2022.
- [43] Junwon Seo, Sangyoon Lee, Kwang In Kim, and Jaeho Lee. In search of a data transformation that accelerates neural field training. In *Proceedings of the IEEE/CVF Conference on Computer Vision and Pattern Recognition (CVPR)*, 2024.
- [44] Kexuan Shi, Xingyu Zhou, and Shuhang Gu. Improved implicit neural representation with fourier bases reparameterized training. *CoRR*, abs/2401.07402, 2024.
- [45] Vincent Sitzmann, Julien N. P. Martel, Alexander W. Bergman, David B. Lindell, and Gordon Wetzstein. Implicit neural representations with periodic activation functions. In *NeurIPS*, 2020.
- [46] Yannick Strümpfer, Janis Postels, Ren Yang, Luc Van Gool, and Federico Tombari. Implicit neural representations for image compression. In *ECCV (26)*, volume 13686 of *Lecture Notes in Computer Science*, pages 74–91. Springer, 2022.
- [47] Matthew Tancik, Ben Mildenhall, Terrance Wang, Divi Schmidt, Pratul P. Srinivasan, Jonathan T. Barron, and Ren Ng. Learned initializations for optimizing coordinate-based neural representations. In *CVPR*, pages 2846–2855. Computer Vision Foundation / IEEE, 2021.
- [48] Matthew Tancik, Pratul P. Srinivasan, Ben Mildenhall, Sara Fridovich-Keil, Nithin Raghavan, Utkarsh Singhal, Ravi Ramamoorthi, Jonathan T. Barron, and Ren Ng. Fourier features let networks learn high frequency functions in low dimensional domains. In *NeurIPS*, 2020.
- [49] Shengjie Wang, Tianyi Zhou, and Jeff A. Bilmes. Bias also matters: Bias attribution for deep neural network explanation. In *ICML*, volume 97 of *Proceedings of Machine Learning Research*, pages 6659–6667. PMLR, 2019.
- [50] Zhou Wang, Alan C. Bovik, Hamid R. Sheikh, and Eero P. Simoncelli. Image quality assessment: from error visibility to structural similarity. *IEEE Trans. Image Process.*, 13(4):600–612, 2004.
- [51] David Wiesner, Julian Suk, Sven Dummer, David Svoboda, and Jelmer M. Wolterink. Implicit neural representations for generative modeling of living cell shapes. In *MICCAI (4)*, volume 13434 of *Lecture Notes in Computer Science*, pages 58–67. Springer, 2022.

- 532 [52] Jelmer M. Wolterink, Jesse C. Zwenenberg, and Christoph Brune. Implicit neural represen-
533 tations for deformable image registration. In *MIDL*, volume 172 of *Proceedings of Machine*
534 *Learning Research*, pages 1349–1359. PMLR, 2022.
- 535 [53] Runzhao Yang. TINC: tree-structured implicit neural compression. In *CVPR*, pages 18517–
536 18526. IEEE, 2023.
- 537 [54] Chen Zhang, Steven Tin Sui Luo, Jason Chun Lok Li, Yik-Chung Wu, and Ngai Wong. Non-
538 parametric teaching of implicit neural representations. In *Forty-first International Conference*
539 *on Machine Learning, ICML 2024, Vienna, Austria, July 21-27, 2024*. OpenReview.net, 2024.
- 540 [55] Richard Zhang, Phillip Isola, Alexei A. Efros, Eli Shechtman, and Oliver Wang. The unreasonable
541 effectiveness of deep features as a perceptual metric. In *CVPR*, pages 586–595. Computer
542 Vision Foundation / IEEE Computer Society, 2018.
- 543 [56] Weixiang Zhang, Shuzhao Xie, Shijia Ge, Wei Yao, Chen Tang, and Zhi Wang. Expansive
544 supervision for neural radiance field. *arXiv preprint arXiv:2409.08056*, 2024.
- 545 [57] Weixiang Zhang, Shuzhao Xie, Chengwei Ren, Shijia Ge, Mingzi Wang, and Zhi Wang.
546 Enhancing implicit neural representations via symmetric power transformation. In *AAAI*, pages
547 10157–10165. AAAI Press, 2025.
- 548 [58] Weixiang Zhang, Shuzhao Xie, Chengwei Ren, Siyi Xie, Chen Tang, Shijia Ge, Mingzi Wang,
549 and Zhi Wang. Evos: Efficient implicit neural training via evolutionary selector. In *Proceedings*
550 *of the IEEE/CVF Conference on Computer Vision and Pattern Recognition (CVPR)*, 2025.
- 551 [59] Allan Zhou, Kaien Yang, Kaylee Burns, Adriano Cardace, Yiding Jiang, Samuel Sokota, J. Zico
552 Kolter, and Chelsea Finn. Permutation equivariant neural functionals. In *NeurIPS*, 2023.